Coupling of a *C*$_2$-Chiral Ferrocene with Phenylalkynyl Groups: Novel Ferrocenophanes Carrying Multiple Chiral Ferrocenyl Units
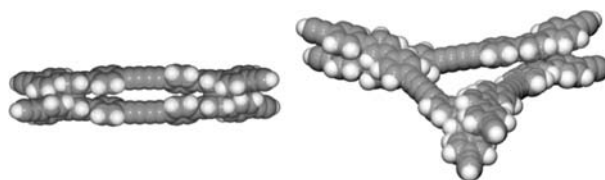
Takahiro Fukino, Norifumi Fujita, and Takuzo Aida*

Department of Chemistry and Biotechnology, School of Engineering, The University of Tokyo, 7-3-1 Hongo, Bunkyo-ku, Tokyo 113-8656, Japan

aida@macro.t.u-tokyo.ac.jp

ABSTRACT

Cyclic Dimer (2)   Cyclic Trimer (3)

Ferrocenophanes with *C*$_2$-Chiral Ferrocenyl Units

Upon treatment with CuCl/TMEDA (1:1) at a high [CuCl]/[1] ratio, enantiopure *C*$_2$-chiral tetrasubstituted ferrocene 1 carrying phenylalkynyl groups is transformed into a novel family of chiral ferrocenophanes 2 and 3 with their ferrocenyl joints connected by a π-conjugated rigid bridge. Compound 3, which is reminiscent of the Escher's endless staircase, is a single conformer with a one-handed helical chirality.

Ferrocene (Fc), an organometallic iron(II) complex with two facing cyclopentadienyl (Cp) ligands, has attracted long-term attention in broad areas of chemistry and materials science because of its chemical stability, redox activity, and aromatic nature.[1] Besides these fundamental features, Fc has been used as a rotary module for molecular machines[2,3] since the Cp ligands in solution undergo a free thermal rotation around the metal center.[4] Likewise, special attention has also been paid for polymers composed of rigid rods and Fc joints,[5] since rotary motions of the joint parts may exert an interesting conformational properties. Being motivated by this idea, we synthesized a novel Fc monomer with phenylalkynyl groups (**1**) for the polymerization via Cu(I)-mediated Glaser−Hay coupling[6] (Scheme 1). A marked feature of monomer **1** is a *C*$_2$ chirality of the Fc part due to its tetrasubstituted structure originally developed as a pivotal module for light-powered molecular scissors.[7] In order to overcome a potential solubility problem of the products, monomer **1** bears trieth-

(1) *Ferrocenes: Ligands, Materials and Biomolecules*; Štěpnička, P., Ed.; Wiley-VCH: Weinheim, 2008.

(2) Kinbara, K.; Muraoka, T.; Aida, T. *Org. Biomol. Chem.* **2008**, *6*, 1871–1876.

(3) (a) Zhang, D.; Zhang, Q.; Su, J.; Tian, H. *Chem. Commun.* **2009**, 1700–1702. (b) Shoji, O.; Okada, S.; Satake, A.; Kobuke, Y. *J. Am. Chem. Soc.* **2005**, *127*, 2201–2210.

(4) Abel, E. W.; Long, N. J.; Orrell, K. G.; Osborne, A. G.; Šik, V. *J. Organomet. Chem.* **1991**, *403*, 195–208.

(5) (a) Choi, T.-L.; Lee, K.-H.; Joo, W.-J.; Lee, S.; Lee, T.-W.; Chae, M. Y. *J. Am. Chem. Soc.* **2007**, *129*, 9842–9843. (b) Engtrakul, C.; Sita, L. R. *Organometallics* **2008**, *27*, 927–937. (c) Baumgardt, I.; Butenschön, H. *Eur. J. Org. Chem.* **2010**, 1076–1087.

(6) (a) Hay, A. S. *J. Org. Chem.* **1960**, *25*, 1275–1276. (b) Siemsen, P.; Livingston, R. C.; Diederich, F. *Angew. Chem., Int. Ed.* **2000**, *39*, 2632–2657.

(7) (a) Muraoka, T.; Kinbara, K.; Kobayashi, Y.; Aida, T. *J. Am. Chem. Soc.* **2003**, *125*, 5612–5613. (b) Muraoka, T.; Kinbara, K.; Aida, T. *Nature* **2006**, *440*, 512–515. (c) Muraoka, T.; Kinbara, K.; Aida, T. *J. Am. Chem. Soc.* **2006**, *128*, 11600–11605. (d) Muraoka, T.; Kinbara, K.; Wakamiya, A.; Yamaguchi, S.; Aida, T. *Chem.—Eur. J.* **2007**, *13*, 1724–1730. (e) Muraoka, T.; Kinbara, K.; Aida, T. *Chem. Commun.* **2007**, 1441–1443. (f) Kai, H.; Nara, S.; Kinbara, K.; Aida, T. *J. Am. Chem. Soc.* **2008**, *130*, 6725–6727.
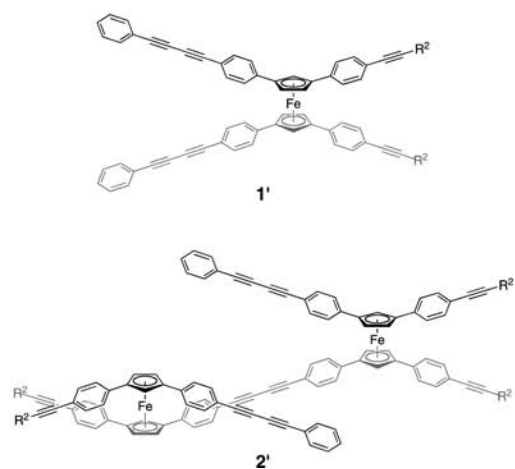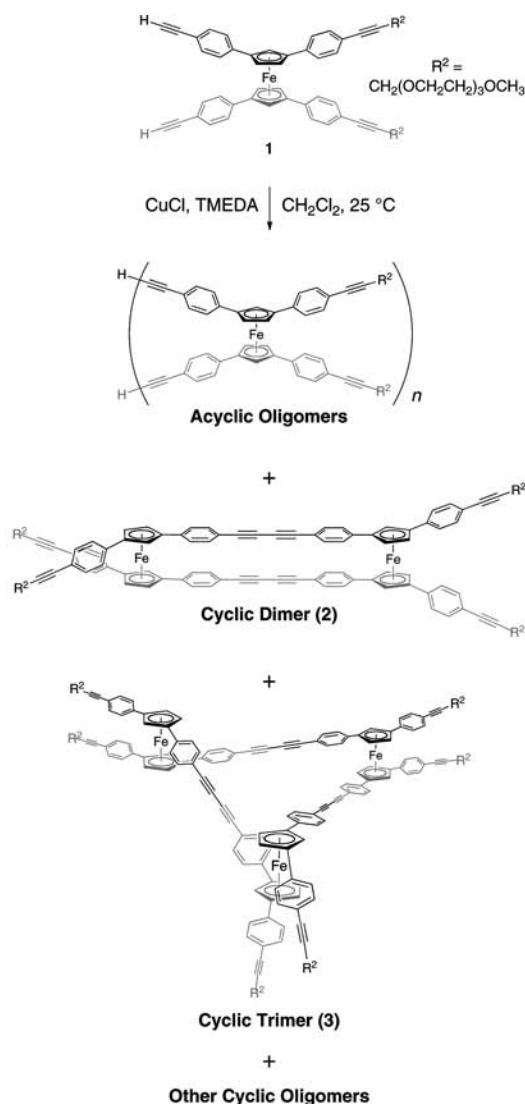
produced (Scheme 1). Although ferrocenophanes with multiple Fc units have been reported,[8] compound **3**, which is reminiscent of the Escher's endless staircase, is the first chiral ferrocenophane with a one-handed helicity.[9]

For the synthesis of a TMS-protected derivative of **1** (**1**$_{TMS}$), a mixture of the meso and racemic forms of 1,1′-bis(4-bromophenyl)-3,3′-bis(4-iodophenyl)ferrocene was subjected to Sonogashira coupling with an acetylene attached to triethylene glycol monomethyl ether and then trimethylsilylacetylene. Preparative chiral HPLC[10a] of the resulting isomeric mixture of **1**$_{TMS}$ (94%) displayed three elution peaks (Figure S13, Supporting Information). The first fraction, corresponding to one of the enantiomers of **1**$_{TMS}$, was collected and subjected to deprotection, affording enantiopure **1** (λ_{max} = 290 nm) almost quantitatively.

As a typical procedure for Glaser−Hay coupling, a CH$_2$Cl$_2$ (1.5 mL) solution of a mixture of enantiopure **1** (21 mg, 0.022 mmol) and CuCl (11 mg, 0.11 mmol) was vigorously stirred under air at 25 °C for 15 min. Then, TMEDA (17 μL, 0.12 mmol) was added, and the mixture was further stirred for 30 min at 25 °C. After acidic workup followed by drying over anhydrous Na$_2$SO$_4$, the resulting solution was filtered with SiO$_2$ and evaporated to dryness. Analytical size-exclusion chromatography (SEC) of the residue showed two elution peaks (Figure 1a). Detailed analysis of the high-
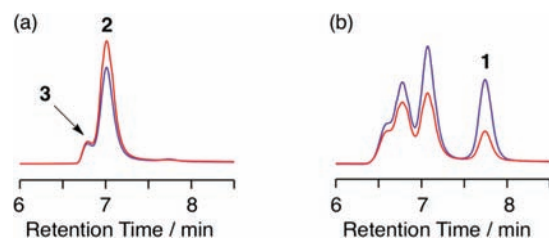
Figure 1. Glaser−Hay coupling of **1** with CuCl/TMEDA (1:1) in CH$_2$Cl$_2$ at 25 °C. Size-exclusion chromatograms (SEC, CHCl$_3$ as an eluent [flow rate 1.0 mL min^{-1}], 25 °C, monitored at 300 (blue) and 350 (red) nm) of the reaction mixtures obtained at [Cu(I)]/[**1**] of (a) 5 after 0.5 h and (b) 0.5 after 18 h.

resolution MALDI-TOF mass spectra of the corresponding fractions, isolated by preparative gel-permeation chromatography (GPC),[10b] revealed that they are cyclic dimer **2** (*m/z*

ylene glycol (TEG) side chains. In the course of this study, we found that, at a high [Cu(I)]/[**1**] ratio, cyclic products (ferrocenophanes) **2** and **3** with defined geometries are

(8) (a) Lippard, S. J.; Martin, G. *J. Am. Chem. Soc.* **1970**, *92*, 7291–7296. (b) Mueller-Westerhoff, U. T. *Angew. Chem., Int. Ed.* **1986**, *25*, 702–717. (c) Mueller-Westerhoff, U. T.; Swiegers, G. F. *Chem. Lett.* **1994**, *23*, 67–68. (d) Grossmann, B.; Heinze, J.; Herdtweck, E.; Köhler, F. H.; Nöth, H.; Schwenk, H.; Spiegler, M.; Wachter, W.; Weber, B. *Angew. Chem., Int. Ed.* **1997**, *36*, 387–389. (e) Southard, G. E.; Curtis, M. D. *Organometallics* **2001**, *20*, 508–522. (f) Dong, G.; Gang, H.; Chun-ying, D.; Ke-liang, P.; Qing-jin, M. *Chem. Commun.* **2002**, 1096–1097. (g) Mizuta, T.; Aotani, T.; Imamura, Y.; Kubo, K.; Miyoshi, K. *Organometallics* **2008**, *27*, 2457–2463. (h) Herbert, D. E.; Gilroy, J. B.; Chan, W. Y.; Chabanne, L.; Staubitz, A.; Lough, A. J.; Manners, I. *J. Am. Chem. Soc.* **2009**, *131*, 14958–14968.
(9) For chiral macrocycles, see, for example: Campbell, K.; Tykwinski, R. R. Chiral Carbon-rich Macrocycles and Cyclophanes. In *Carbon-Rich Compounds: From Molecules to Materials*; Haley, M. M., Tykwinski, R. R., Eds.; Wiley-VCH: Weinheim, 2006; Chapter 6, pp 229−294.
(10) (a) Chiralpak IB, hexane/EtOH (4/1 v/v). (b) Bio-Beads, CHCl$_3$.

calcd for $C_{116}H_{112}Fe_2O_{16}$ [M$^+$] 1872.6649, obsd 1872.6710; Figure S14a, Supporting Information) and trimer **3** (*m/z* calcd for $C_{174}H_{168}Fe_3O_{24}$ [M$^+$] 2808.9974, obsd 2809.0021; Figure S14b, Supporting Information). The isolated yields of **2** and **3** were 38 and 15%, respectively, which are in agreement with those evaluated from Figure 2b. In contrast, when the
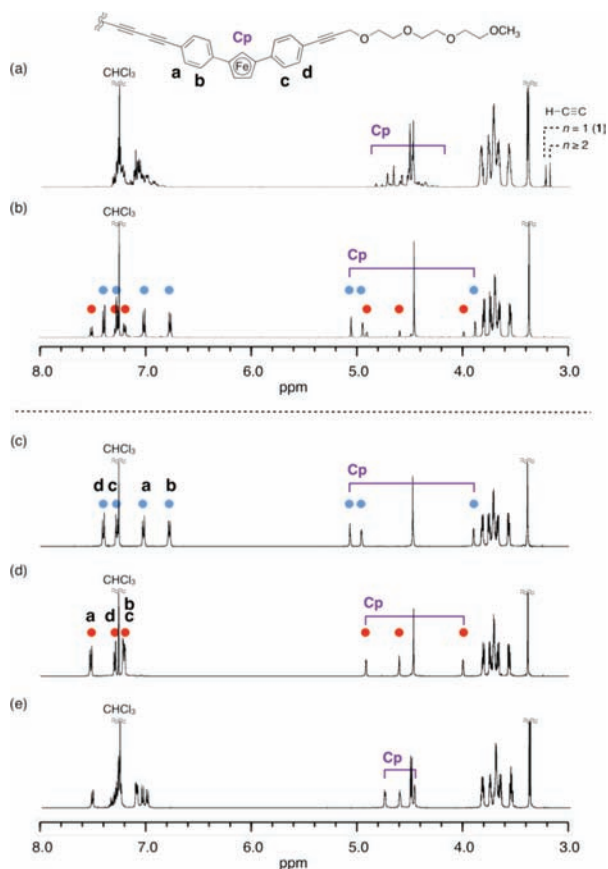

Figure 2. ¹H NMR spectra of the reaction mixtures obtained at [Cu(I)]/[**1**] of (a) 0.5 after 18 h and (b) 5 after 0.5 h, along with that of cyclic (c) **2**, (d) **3**, and (e) acyclic **2'** in CDCl₃ at 20 °C.

molar ratio [CuCl]/[**1**] was decreased to one-tenth that employed for the above reaction conditions, a much different SEC profile resulted (Figure 1b). ¹H NMR spectroscopy indicated that the reaction mixture includes neither **2** nor **3** but linear oligomers along with **1** unreacted (Figure 2a). The observed dependence of product selectivity on the molar ratio [CuCl]/[**1**] may be reasonable, considering that the cyclization of acyclic precursors can occur only when their two termini are activated simultaneously.[6]

As expected, ¹H NMR spectra of ferrocenophanes **2** (Figure 2c) and **3** (Figure 2d) in CDCl₃ did not show any signal assignable to H–C≡C– characteristic of acyclic analogues (e.g., δ 3.18 for **1** in Figure S6, Supporting Information). Noteworthy, their spectral profiles were essentially different from that of reference acyclic dimer **2'** (Scheme 1, Figure 2e). For example, cyclic dimer **2** in the aromatic region showed two sets of doublet signals (Figure 2c), where the paired doublets at δ 6.78 and 7.02 are upfield-

shifted from the other (δ 7.28 and 7.40). With the aid of 2D NMR spectroscopy (Figures S15 and S16, Supporting Information), the former set was assigned to ArH in the bridging aromatic units that are perfectly eclipsed with one another, while the latter originates from the exocyclic (peripheral) aromatic units attached to the alkynyl-TEG chains. It should be noted that the three Cp signals spread over a rather wide chemical shift range from δ 3.9 to 5.1, where one of them is remarkably upfield shifted by 1.1 ppm from the other. In sharp contrast, its acyclic reference **2'** displayed just an ordinary spectral feature both for the aromatic and Fc regions (Figure 2e), where the chemical shift range of the Cp signals, for example, is only 0.3 ppm. On the other hand, in case of cyclic trimer **3** (Figure 2d), the three Cp signals spread over the chemical shift range (0.9 ppm) as wide as that observed for cyclic **2**, whereas all the ArH signals, except one at δ 7.5, appeared in a very narrow range of δ 7.2–7.3. Here, one may draw several different conformations for the cyclic trimer. However, the spectral pattern of **3** is quite simple, displaying only four doublet signals due to ArH. Hence, **3** is obviously a single conformer adopting a highly symmetric geometry, i.e., helical structure with a symmetry group D_3. Considering that its C_2-chiral Fc joints all adopt an identical absolute configuration, only two helical conformers **3A** and **3B** with opposite handednesses are possible (Figure 3). By means of 2D NMR
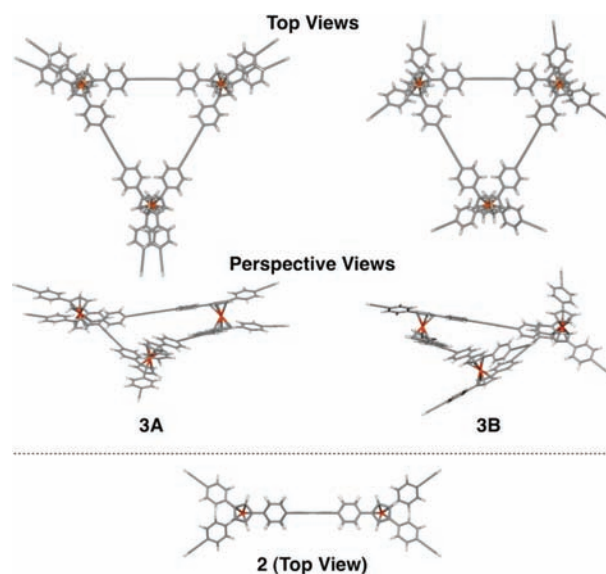
Figure 3. Optimized structures (B3LYP/6-31G*) of **2** and two possible helical conformers of cyclic trimer **3**. TEG chains are not taken into account for optimization.

spectroscopy (Figures S17 and S18, Supporting Information), all four ArH signals were successfully assigned as shown in Figure 2d. It is noteworthy that the exocyclic Ar protons c and d in **3** are more shielded than those in **2**, indicating that these Ar units are in closer proximity to one another than in the case of **2** (Figure 3, bottom). Namely, **3B** can be excluded, leaving **3A** as the most likely candidate.
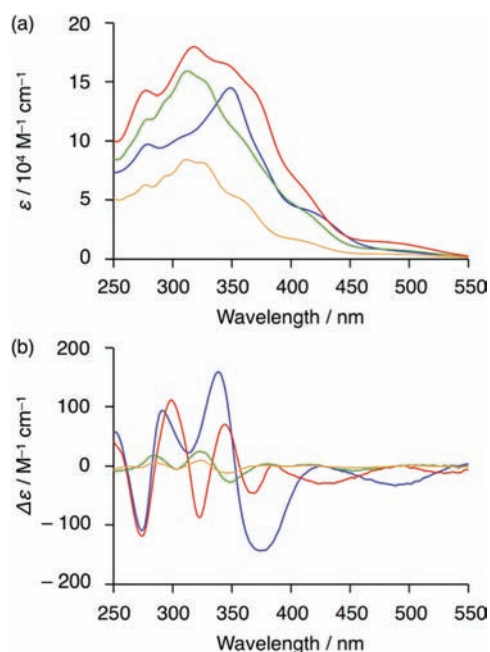
Figure 4. (a) Electronic absorption and (b) circular dichroism (CD) spectra in CH_2Cl_2 at 20 °C of cyclic **2** (blue) and **3** (red), along with those of acyclic references **1′** (orange) and **2′** (green).

As shown in Figure 4a, not only acyclic references **1′** (orange) and **2′** (green) but also cyclic compounds **2** (blue) and **3** (red), in CH_2Cl_2 at 20 °C, displayed a broad absorption band up to wavelengths longer than 500 nm. Whereas the spectral shape of triangular **3** is similar to those of acyclic **1′** and **2′**, cyclic dimer **2** (blue) showed a peculiar spectral feature with a red-shifted absorption maximum at 350 nm. This band most likely originates from the fully eclipsed π-conjugated bridges with a parallel orientation across the ferrocenyl joints. Figure 4b showed circular dichroism (CD) spectra of the above four compounds in CH_2Cl_2 at 20 °C. Monomer **1**, though enantiomerically pure, was substantially CD-silent. Likewise, the chiroptical activity of **1′** (orange) is rather small. Although acyclic dimer **2′** (green) has an enhanced absorption spectral feature (Figure 4a), its CD activity (Figure 4b) is just twice as large as that of **1′**. In sharp contrast, cyclic **2** (blue) displayed highly intense CD bands over the entire absorption range. The same was true for cyclic **3** (red), although the spectral shape was quite different from that of **2** (blue). Here it should be noted that the intensity of an exciton-coupled CD band depends on the dihedral angle of transition dipoles involved.[11] Thus, the weak chiroptical features of acyclic **1′** (orange) and **2′** (green)

suggest that the geometries of their major conformers are analogous to neither **2** nor **3**. This indication can be supported by the large ^{1}H NMR spectral difference in the Cp region between the cyclic and acyclic oligomers in Figure 2.

Both cyclic and acyclic compounds underwent reversible oxidation. In cyclic voltammetry using Pt working/counter electrodes at 25 °C (0.1 M Bu_4NPF_6 in CH_2Cl_2), all of the compounds, irrespective of the numbers of chromophores and Fc joints, displayed a single oxidation wave, indicating that the cationic species in their oxidation states is mostly localized in a Fc joint.[12] Although the oxidation potentials ($E_{1/2}$/V versus Fc/Fc^+) are not much different from one another, cyclic **2** (+0.16) and **3** (+0.19) are slightly less subject to oxidation than acyclic **1′** (+0.13) and **2′** (+0.13).

In conclusion, by employing a high [CuCl]/[**1**] ratio, Glaser−Hay coupling of enantiopure C_2-chiral ferrocene **1** bearing phenylalkynyl groups proceeds to give cyclic oligomers **2** and **3** as major isolable products. These compounds are the first ferrocenophanes that bear multiple C_2-chiral ferrocenyl units in a predetermined manner.[8e] Compound **3** is reminiscent of the Escher's endless staircase. Of interest, this triangular helical molecule is formed as a single conformer (**3A** in Figure 3) with a one-handed helical chirality. While cyclic compounds **2** and **3** display a large chiroptical activity, acyclic references **1′** and **2′** are much less. Together with the large ^{1}H NMR spectral difference in the Cp region between the cyclic and acyclic compounds, major conformers of the acyclic compounds are geometrically different from **2** and **3**. Conformational and CD spectral studies on discrete linear oligomers of **1** with larger numbers of the repeating units are interesting subjects worthy of further investigation.

Supporting Information Available: Synthesis of **1**, **1′**, and **2′**. Isolation and MALDI-TOF mass/NMR data of **2** and **3**. Details for computational optimization of the model compounds of **2** and **3**. This material is available free of charge via the Internet at http://pubs.acs.org.

OL1010714

(11) Aimi, J.; Nagamine, Y.; Tsuda, A.; Muranaka, A.; Uchiyama, M.; Aida, T. *Angew. Chem., Int. Ed.* **2008**, *47*, 5153–5156.

(12) For electronic communication between Fc units linked by a π-conjugated bridge, see, for example: (a) Wong, W.-Y.; Ho, K.-Y.; Ho, S.-L.; Lin, Z. *J. Organomet. Chem.* **2003**, *683*, 341–353. (b) Altmann, M.; Friedrich, J.; Beer, F.; Reuter, R.; Enkelmann, V.; Bunz, U. H. F. *J. Am. Chem. Soc.* **1997**, *119*, 1472–1473. (c) Kurosawa, M.; Nankawa, T.; Matsuda, T.; Kubo, K.; Kurihara, M.; Nishihara, H. *Inorg. Chem.* **1999**, *38*, 5113–5123. (d) Diallo, A. K.; Daran, J.-C.; Varret, F.; Ruiz, J.; Astruc, D. *Angew. Chem., Int. Ed.* **2009**, *48*, 3141–3145.